Research Journal of Applied Sciences, Engineering and Technology 8(13): 1510-1521, 2014
DOI:10.19026/rjaset.8.1129
ISSN: 2040-7459; e-ISSN: 2040-7467

Submitted: May 07, 2014 Accepted: June 08, 2014 Published: October 05, 2014

Research Article

An Insight into the Time Domain Phenomenon during the Transition Zone from Induction Motor to Synchronous Motor Mode for a Current Source Inverter Fed Synchronous Motor Drive System

A.B. Chattopadhyay and Sunil Thomas
Department of Electrical and Electronics Engineering, Birla Institute of Technology and Science, Pilani-Dubai Campus, P.O. Box 345055, Plot No. UG 06, Dubai International Academic City, Dubai, U.A.E

Abstract: Modeling of synchronous motor plays a dominant role in designing complicated drive system for different applications, especially large blower fans etc., for steel industries. As synchronous motor has no inherent starting torque generally it is started as an induction motor with the help of a damper winding and it pulls into synchronism under certain conditions. The present study exactly concentrates on this particular zone of transition from induction motor to synchronous motor mode for a current source inverter fed synchronous motor drive system. Due to complexity of synchronous motor in terms of number of windings and finite amount of air gap saliency, direct modeling of such transition zone in time domain becomes cumbersome at the first instance of modeling. That is why firstly the modeling is presented in complex frequency domain and then the time domain modeling is obtained by applying inverse Laplace transform technique. Apparently it seems to be a straight forward mathematical treatment but involvement of Convolution Integral for converting the formulation from s-domain to time domain becomes a matter of interest and it may draw the attention of various researchers working in this area. Furthermore the time domain response of the disturbance function may help a designer to fix up the time instant when the pull in phenomenon will be imposed by throwing the field winding to a DC supply.

Keywords: Computer simulation, current source inverter, induction motor, small perturbation model, starting transients, synchronous machine

INTRODUCTION

Many constant speed applications such as fans, fuel pump and compressors comprising a considerable amount of total electrical appliances (Isfahani and Vaez-Zadeh, 2011) basically need a 3 phase synchronous motor. Even though permanent magnet synchronous motors are widely used in such applications, current source inverter fed normal synchronous motors can also be applied in many constant speed applications (Knight and McClay, 2000; Weifu *et al*., 2012). The steady state stability study of a current source inverter fed synchronous motor was basically initiated in 1974 (Gordon *et al*., 1974) and after this as an extension, Chattopadhyay *et al*. (2011) presented a detailed analysis of a current source inverter fed synchronous motor drive system taking damper windings into account in 2011. So far the research accuracy of the paper by Chattopadhyay *et al*. (2011) is covered; it is not clear that exactly what is happening in the transition zone when the machine is jumping from induction motor action to synchronous motor action. Again the concentration on such detailed aspect is a matter of long discussion and in this context many researchers have tried to put sufficient light on the matter. The research paper (Ma *et al*., 2006) explains the analysis of magnetic fields and temperature fields for a salient pole synchronous motor in the process of steady state. They have used the d-q model of the synchronous motor but the role of field winding in transition from induction motor to synchronous motor is not reflected in the mathematical model.

A similar observation is valid on the other work (Wang and Ren, 2003) and it represents a good state variable model and its mathematic simulations in time domain. The research paper (Sergelen, 2007; Najafi and Kar, 2007) carries important works on the mathematical modeling of a salient pole synchronous motor supplied by a frequency converter and also the effect of short circuit voltage profile on the transient performance of permanent magnet synchronous motors. An important work on non-linear control of an inverter motor drive system with input filter (Marx *et al*., 2008) draws attention. In this study the author has given a detailed signal analysis of the DC-link voltage stability.

Another interesting paper by Das and Casey (1999) and Al-Ohaly *et al*. (1997) clearly portrays the critical aspects of starting a large synchronous motor. Even

Corresponding Author: Sunil Thomas, Department of Electrical and Electronics Engineering, Birla Institute of Technology and Science, Pilani-Dubai Campus, U.A.E, Tel.: (009714) 4200700 extn. 408; Fax: (009714) 4200555

though this particular study does not involve much mathematical analysis but the range of the slip presented in this study with reference to pull in torque of a synchronous motor really may help a designer to select a particular synchronous motor for any specific application.

Based on the above said literature review, to the best of the authors understanding it reveals that researchers have not put sufficient light on the fact that exactly what happens to the mathematical model of a synchronous motor in time domain or complex frequency domain during the period when field winding is disconnected from the external resistance (generally 6-7 times of main field winding resistance to avoid effects due to George's phenomenon) and immediately thrown to the DC source. Basically the formulation will be done in complex frequency domain involving two transformed quantities:

- Small perturbation in load torque
- Small perturbation in field angle

This is a traditional technique of formulation to put some light on the overall modeling of synchronous motor and also on the steady state aspects in general and transient state analysis in particular. But in the present problem as the machine's transition from induction motor mode to synchronous motor mode is of prior importance. A disturbance function in complex frequency domain is expected to appear in the resultant formulation and it is expected to disturb the linkup between the above said two transformed quantities (field angle and load torque). It is quite natural that the modeling of the disturbance function in complex frequency domain will give a lot of information to the design of a synchronous motor applied to various drive system, but still the necessity of getting the time domain response of that disturbance function remain within the scope of the research. Hence to get the time domain behavior of that disturbance function becomes the main objective of the authors of the present paper; because it will give more detailed information regarding the convergence and divergence nature of the disturbing function such that a designer can pre assume what should be the time zone for synchronizing the motor into pull-in phenomenon.

MATERIALS AND METHODS

The basic block diagram of the proposed scheme is shown in Fig. 1.

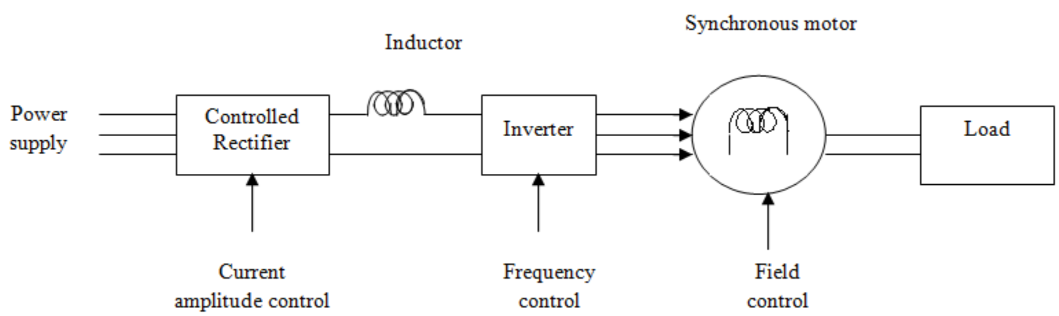

Fig. 1: Drive configuration for open-loop current-fed synchronous motor control

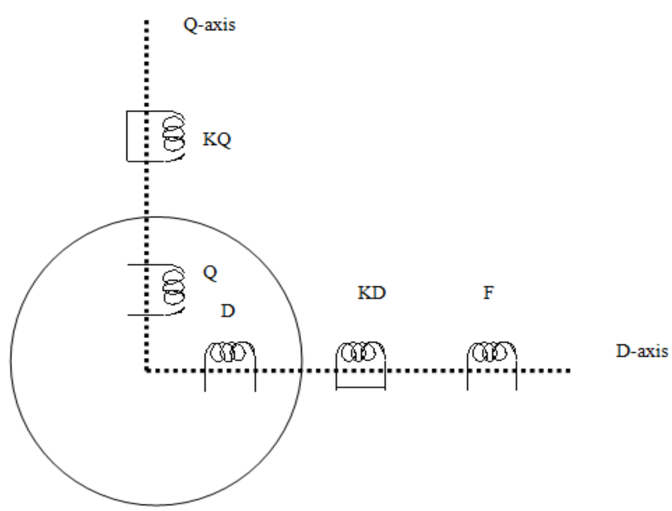

Fig. 2: Primitive machine model of a synchronous motor

To have a better feeling of the method of analysis, the primitive machine model of the synchronous motor is drawn and it is shown in Fig. 2.

In the following analysis, saturation is ignored but provision is made for inclusion of saliency and one number of damper winding on each axis. Following Park's transform, a constant stator current of value is at a field angle 'β' can be represented by direct and quadrature axis currents as:

$$i_d = i_s \cos\beta \tag{1}$$

$$i_q = i_s \sin\beta \tag{2}$$

Designating steady state value by the subscript '0' and small perturbation by Δ, the perturbation equations of the machines are:

$$\Delta i_d = -i_s \sin\beta_0 \Delta\beta \tag{3}$$

$$\Delta i_q = i_s \cos\beta_0 \Delta\beta \tag{4}$$

The transformed version of Eq. (3) and (4) are:

$$\Delta I_d(s) = -i_s \sin\beta_0 \Delta\beta(s) \tag{5}$$

$$\Delta I_q(s) = i_s \cos\beta_0 \Delta\beta(s) \tag{6}$$

The generalized expression for electromagnetic torque of a primitive machine model is an established one and it is expressed as:

$$\begin{aligned} T_e &= \Psi_d i_q - i_d \Psi_q \\ &= \left(L_d i_d + L_{md} i_f + L_{md} i_{kd}\right) i_q - \left(L_q i_q + L_{mq} i_{kq}\right) i_d \\ &= \left(L_d - L_q\right) i_d i_q + L_{md} i_q i_f + L_{md} i_{kd} i_q - L_{mq} i_{kq} i_d \end{aligned} \tag{7}$$

Small signal version of torque equation in time domain is expressed as:

$$\begin{aligned} \Delta T_e = &\left(L_d - L_q\right) \Delta i_d i_{q0} + \left(L_d - L_q\right) \Delta i_q i_{d0} + L_{md} \Delta i_q i_{f0} + L_{md} \Delta i_f i_{q0} \\ &+ L_{md} \Delta i_{kd} i_{q0} + L_{md} i_{kd0} \Delta i_q - L_{mq} \Delta i_{kq} i_{d0} - L_{mq} i_{kq0} \Delta i_d \end{aligned} \tag{8}$$

Equation (8) after being transformed takes the shape as given by:

$$\begin{aligned} \Delta T_e(s) = &\left(L_d - L_q\right) i_{q0} \Delta I_d(s) + \left(L_d - L_q\right) i_{d0} \Delta I_q(s) + L_{md} i_{f0} \Delta I_q(s) + L_{md} i_{q0} \Delta I_f(s) \\ &+ L_{md} i_{q0} \Delta I_{kd}(s) + L_{md} i_{kd0} \Delta I_q(s) - L_{mq} i_{d0} \Delta I_{kq}(s) - L_{mq} i_{kq0} \Delta I_d(s) \\ = &[\left(L_d - L_q\right) i_{q0} - L_{mq} i_{kq0}] \Delta I_d(s) + \left[\left(L_d - L_q\right) i_{d0} + L_{md} i_{kd0} + L_{md} i_{f0}\right] \Delta I_q(s) \\ &+ L_{md} i_{q0} \Delta I_f(s) + L_{md} i_{q0} \Delta I_{kd}(s) - L_{mq} i_{d0} \Delta I_{kq}(s) \end{aligned} \tag{9}$$

To tackle Eq. (9) in an easier form, it is expressed as:

$$\Delta T_e(s) = c_1 \Delta I_d(s) + c_2 \Delta I_q(s) + c_3 \Delta I_f(s) + c_4 \Delta I_{kd}(s) + c_5 \Delta I_{kq}(s) \tag{10}$$

where,

$$c_1 = \left[\left(L_d - L_q\right) i_{q0} - L_{mq} i_{kq0}\right] \tag{11}$$

$$c_2 = \left[\left(L_d - L_q \right) i_{d0} + L_{md} i_{kd0} + L_{md} i_{f0} \right] \tag{12}$$

$$c_3 = L_{md} i_{q0} \tag{13}$$

$$c_4 = L_{md} i_{q0} \tag{14}$$

$$c_5 = -L_{mq} i_{d0} \tag{15}$$

The small perturbation model of the transformed voltage balance equations of F-coil, KD-coil and KQ are expressed as:

$$\frac{c}{s} + s_1 \frac{k}{s} = \Delta U_f(s) = R_f \Delta I_f(s) + sL_{ff} \Delta I_f(s) + sL_{md} \Delta I_d(s) + sL_{md} \Delta I_{kd}(s) \tag{16}$$

where, c = 220 Volts, S_1 = slip and k = (N_f/Na)*(415/√3)
N_f = Number of turns in field winding
Na = Number of turns in armature winding:

$$0 = \Delta U_{kd}(s) = R_{kd} \Delta I_{kd}(s) + sL_{kkd} \Delta I_{kd}(s) + sL_{md} \Delta I_d(s) + sL_{md} \Delta I_f(s) \tag{17}$$

$$\Delta U_{kq}(s) = R_{kq} \Delta I_{kq}(s) + sL_{kkq} \Delta I_{kq}(s) + sL_{mq} \Delta I_q(s) \tag{18}$$

where, c = 220 Volts, S_1 = slip and k = (N_f/Na)*(415/√3)
N_f = Number of turns in field winding
Na = Number of turns in armature winding

As the damper winding on d-axis and q-axis are short-circuited within themselves, $\Delta U_{kd} = 0$ and $\Delta U_{kq} = 0$. So in transformed version ΔU_{kd} (s) = 0 and ΔU_{kq} (s) = 0 as shown in Eq. (17) and (18). Furthermore in general, the voltage fed to the field winding is fixed. It is a well known fact that a synchronous motor cannot start for itself and the easiest way to start a synchronous motor is to start it as an induction machine with the help of damper windings. But the problem is that we have to investigate what will be status of field winding of the synchronous motor when the damper winding is in action. As already the winding was physically embedded (existing) and during the running of the machine one cannot take it out. In other words when damper winding is in action field winding effect has to be inactivated. Such inactivation may be done by the following methods:

- Field winding completely Open Circuit
- Field Winding Short Circuit in itself

The status of field winding in (a) can be looked upon as a transformer whose primary winding constitutes of 3 phase armature winding supplied from 415V (L-L) ac and whose secondary winding is the field winding being open circuited. As generally in a normal synchronous machine of normal design N_f/N_a>>1, where N_f is number of field windings and N_a is number of armature windings. The induced voltage in the open field terminal will be large and it may lead to hazardous conduction so far as operator safety is concerned. Hence this case is rejected.

Status of the field winding in (b): The induced emf in field winding due to transformer action will produce a single phase alternating current and in turn will produce a pulsating field in field winding. It is well known that a pulsating field m.m.f can be resolved as a combination of forward rotating and backward rotating m.m.f magnetic fields (strengths of each resolved component is half of the original pulsating m.m.f). The effect of backward rotating magnetic field will produce a torque opposite to the (asynchronous/induction) motor torque and it will dominate at some value of slip. Hence a situation may arise and motor may stall due to the negative effect of backward component. This phenomenon is known as George's phenomenon.

Hence such case cannot be completely accepted. However there is some remedial method. The field winding may be closed through an external resistance which is about 6-7 times of original field resistance; such that the magnitude of short circuit current diminishes and as a result effect of resolved backward component will be less or reduced.
What happens to change on field voltage (ΔU_f).

In the current research problem ΔU_f cannot be equal to zero because originally it was an induction motor with the field winding short circuited in it or closed through an external resistance of large value and at a later stage it was pulled into synchronism when dc supply is fed to the winding.

Quantitatively, ΔU_f should depend on a particular property of induction motor and that property must be 'SLIP'. Here the technique of mathematical modeling appears as a novel approach and this approach forms the foundation of the proposed analysis. The proposed modeling considers that field winding is closed within itself. In other words the presence of external large resistance has not been considered in modeling to make the mathematical treatment comparatively easy. However it does not affect the accuracy of the system as the external resistance can be lumped or clubbed with the field winding.

From Eq. (16) and (17) it yields:

$$\Delta I_f(s) = \left(\frac{s^2(L_{md}{}^2 - L_{md}L_{kkd}) - sL_{md}R_{kd}}{s^2(L_{kkd}L_{ff} - L_{md}{}^2) + s(L_{kkd}R_f + R_{kd}L_{ff}) + R_{kd}R_f} \right) \Delta I_d(s) - \mathrm{F}_{32}(\mathrm{s}) \tag{19}$$

where,

$$\mathrm{F}_{32}(\mathrm{s}) = (R_{kd} + sL_{kkd})[\frac{c + s_1 k}{s^2 L_{md}}] \tag{20}$$

Similarly Eq. (16) and (17) yields:

$$\Delta I_{kd}(s) = F_{31}(s) - \left(\frac{s^2(L_{md}{}^2 - L_{md}L_{ff}) - sL_{md}R_f}{s^2(L_{kkd}L_{ff} - L_{md}{}^2) + s(L_{kkd}R_f + R_{kd}L_{ff}) + R_{kd}R_f} \right) \Delta I_d(s) = F_{31}(s) - \left(\frac{d_1 s^2 + d_2 s}{D(s)} \right) \Delta I_d(s) \tag{21}$$

where,

$$F_{31}(s) = \frac{\mathrm{c} + \mathrm{s_1 k}}{s^2} \left[1 - \left\{ \left(\frac{R_f}{SL_{md}} + \frac{L_{ff}}{L_{md}} \right) \left(R_{kd} + sL_{kkd} \right) \right\} \right] \tag{22}$$

$$\mathrm{d_1} = \left(\mathrm{L_{md}}^2 - \mathrm{L_{md}L_{ff}} \right) \tag{23}$$

$$\mathrm{d_2} = -\mathrm{L_{md}R_f} \tag{24}$$

From Eq. (18) it is obtained:

$$\Delta I_{kq}(s) = \left(\frac{-sL_{mq}}{R_{kq} + sL_{kkq}} \right) \Delta I_q(s) \tag{25}$$

$$= \left(\frac{e_1 s}{Q(s)} \right) \Delta I_q(s) \tag{26}$$

where,

$$\mathrm{e_1} = -\mathrm{L_{mq}} \tag{27}$$

$$\mathrm{Q(s)} = \mathrm{f_1 s} + \mathrm{f_2} \tag{28}$$

$$\mathrm{f_1} = \mathrm{L_{kkq}} \tag{29}$$

$$\mathrm{f_2} = \mathrm{R_{kq}} \tag{30}$$

Substituting Eq. (19), (21) and (25) in (10), it yields:

$$\Delta T_e(s) = c_1 \Delta I_d(s) + c_2 \Delta I_q(s) + c_3 \left[\frac{a_1 s^2 + a_2 s}{D(s)} \right] \Delta I_d(s) + c_4 \left[\frac{d_1 s^2 + d_2 s}{D(s)} \right] \Delta I_d(s) + c_5 \left[\frac{e_1 s}{Q(s)} \right] \Delta I_q(s)$$

$$= \left[c_1 + \frac{c_3 a_1 s^2 + c_3 a_2 s + c_4 d_1 s^2 + c_4 d_2 s}{D(s)} \right] \Delta I_d(s) + \left[c_2 + \frac{c_5 e_1 s}{Q(s)} \right] \Delta I_q(s) + \mathrm{F}_3(\mathrm{s}) \quad (31)$$

where,

$$\mathrm{F}_3(\mathrm{s}) = \mathrm{F}_{31}(\mathrm{s}) - \mathrm{F}_{32}(\mathrm{s}) \quad (32)$$

Equation (31) can be re expressed as:

$$\Delta T_e(s) = \left[\frac{(m_1 s^3 + m_2 s^2 + m_3 s + m_4) \Delta I_d(s) + (n_1 s^3 + n_2 s^2 + n_3 s + n_4) \Delta I_q(s)}{l_1 s^3 + l_2 s^2 + l_3 s + l_4} \right] + \mathrm{F}_3(\mathrm{s}) \quad (33)$$

where,

$$\mathrm{m}_1 = \mathrm{f}_1 \mathrm{c}_1 \mathrm{b}_1 + \mathrm{c}_3 \mathrm{a}_1 \mathrm{f}_1 + \mathrm{c}_4 \mathrm{d}_1 \mathrm{f}_1 \quad (34)$$

$$\mathrm{m}_2 = \mathrm{c}_1 \mathrm{f}_1 \mathrm{b}_2 + \mathrm{c}_3 \mathrm{a}_2 \mathrm{f}_1 + \mathrm{c}_4 \mathrm{d}_2 \mathrm{f}_1 + \mathrm{c}_1 \mathrm{b}_1 \mathrm{f}_2 + \mathrm{c}_3 \mathrm{a}_1 \mathrm{f}_2 + \mathrm{c}_4 \mathrm{d}_1 \mathrm{f}_2 \quad (35)$$

$$\mathrm{m}_3 = \mathrm{c}_1 \mathrm{b}_2 \mathrm{f}_2 + \mathrm{c}_3 \mathrm{a}_2 \mathrm{f}_2 + \mathrm{c}_4 \mathrm{d}_2 \mathrm{f}_2 + \mathrm{c}_1 \mathrm{b}_3 \mathrm{f}_1 \quad (36)$$

$$\mathrm{m}_4 = \mathrm{c}_1 \mathrm{b}_3 \mathrm{f}_2 \quad (37)$$

$$\mathrm{n}_1 = \mathrm{f}_1 \mathrm{c}_2 \mathrm{b}_1 + \mathrm{c}_5 \mathrm{e}_1 \mathrm{b}_1 \quad (38)$$

$$\mathrm{n}_2 = \mathrm{c}_2 \mathrm{f}_2 \mathrm{b}_1 + \mathrm{c}_2 \mathrm{f}_1 \mathrm{b}_2 + \mathrm{c}_5 \mathrm{e}_1 \mathrm{b}_2 \quad (39)$$

$$\mathrm{n}_3 = \mathrm{c}_2 \mathrm{f}_2 \mathrm{b}_2 + \mathrm{b}_3 \mathrm{c}_2 \mathrm{f}_1 + \mathrm{b}_3 \mathrm{c}_5 \mathrm{e}_1 \quad (40)$$

$$\mathrm{n}_4 = \mathrm{c}_2 \mathrm{f}_2 \mathrm{b}_3 \quad (41)$$

$$\mathrm{l}_1 = \mathrm{b}_1 \mathrm{f}_1 \quad (42)$$

$$\mathrm{l}_2 = \mathrm{b}_2 \mathrm{f}_1 + \mathrm{b}_1 \mathrm{f}_2 \quad (43)$$

$$\mathrm{l}_3 = \mathrm{b}_3 \mathrm{f}_1 + \mathrm{b}_2 \mathrm{f}_2 \quad (44)$$

$$\mathrm{l}_4 = \mathrm{b}_3 \mathrm{f}_2 \quad (45)$$

Substituting the expressions for $\Delta \mathrm{I_d}(\mathrm{s})$ and $\Delta \mathrm{I_q}(\mathrm{s})$ from Eq. (3) and (4) in (33), we have:

$$\Delta T_e(s) = \left[\frac{(m_1 s^3 + m_2 s^2 + m_3 s + m_4)(-i_s \sin \beta_0(s)) + (n_1 s^3 + n_2 s^2 + n_3 s + n_4)(i_s \cos \beta_0(s))}{l_1 s^3 + l_2 s^2 + l_3 s + l_4} \right] \Delta \beta(s) + \mathrm{F}_3(\mathrm{s}) \quad (46)$$

Equation (46) can be re-expressed as:

$$\Delta T_e(s) = \left[\frac{x_1 s^3 + x_2 s^2 + x_3 s + x_4}{l_1 s^3 + l_2 s^2 + l_3 s + l_4}\right]\Delta\beta(s) + F_3(s) \tag{47}$$

$$\Delta T_e(s) = T_1(s)\Delta\beta(s) + F_3(s) \tag{48}$$

where,

$$T_1(s) = \left[\frac{x_1 s^3 + x_2 s^2 + x_3 s + x_4}{l_1 s^3 + l_2 s^2 + l_3 s + l_4}\right] \tag{49}$$

$$x_1 = n_1 i_s \cos\beta_0 - m_1 i_s \sin\beta_0 \tag{50}$$

$$x_2 = n_2 i_s \cos\beta_0 - m_2 i_s \sin\beta_0 \tag{51}$$

$$x_3 = n_3 i_s \cos\beta_0 - m_3 i_s \sin\beta_0 \tag{52}$$

$$x_4 = n_4 i_s \cos\beta_0 - m_4 i_s \sin\beta_0 \tag{53}$$

The torque dynamic equation of a synchronous motor can be written as:

$$T_e - T_L = J\frac{d\omega}{dt} \tag{54}$$

where,
ω = Motor speed in mechanical rad./sec
J = Polar moment of inertia of motor and load (combined)

The small change in speed 'ω' equal to Δω can be related to small change in field angle, Δβ as given by:

$$\Delta\omega = -\frac{d(\Delta\beta)}{dt} \tag{55}$$

The negative sign in equation physically indicates a drop in speed (ω) due to increase in field angle (β). Based on Eq. (55), the following expression can be written:

$$J\frac{d(\Delta\omega)}{dt} = J\frac{d}{dt}\left[-\frac{d}{dt}(\Delta\beta)\right] = -J\frac{d^2}{dt^2}(\Delta\beta) \tag{56}$$

The small-perturbation model of Eq. (54) can be written as:

$$\Delta T_e - \Delta T_L = J\frac{d(\Delta\omega)}{dt} \tag{57}$$

Combining Eq. (56) and (57), it yields:

$$\Delta T_e - \Delta T_L = -J\frac{d^2}{dt^2}(\Delta\beta) \tag{58}$$

The transformed version of Eq. (58), with initial condition relaxed, comes out to be:

$$T_e(s) - T_L(s) = -Js^2\Delta\beta(s) \tag{59}$$

Substituting the expression for $\Delta T_e(s)$ from Eq. (47) in (59), we have:

$$T_1(s)\Delta\beta(s) + Js^2\Delta\beta(s) + \mathrm{F}_3(\mathrm{s}) = \Delta T_L(s) \tag{60}$$

$$\frac{1}{\left[T_1(s)+Js^2\right]}\Delta T_L(s) - \frac{1}{\left[T_1(s)+Js^2\right]}\mathrm{F}_3(\mathrm{s}) = \Delta\beta(s) \tag{61}$$

The block diagram representation of the system obtained from the above equation is shown in Fig. 3.
The disturbance function can be taken separately and a detailed analysis in time domain is carried out as follows:

$$D(\mathrm{s}) = \frac{F_3(\mathrm{s})}{T_1(s)+Js^2} \tag{62}$$

$$F_3(s) = \frac{-c_1}{s} + \frac{c_2}{s^2} - \frac{c_3}{s^3} - \frac{c_4}{s^2} - \frac{c_5}{s}$$
$$= \frac{-(c_1+c_5)}{s} + \frac{(c_2-c_4)}{s^2} - \frac{c_3}{s^3} \tag{63}$$

$$F_3(\mathrm{t}) = -(c_1+c_5)u(\mathrm{t}) + (\mathrm{c}_2-\mathrm{c}_4)\,\mathrm{t} - \frac{\mathrm{c}_3}{2}t^2$$
$$= -1.4588*10^3 + 543.0379t - 0.0127t^2 \tag{64}$$

$$Denominator = Q(s)\ \frac{1}{T_1(\mathrm{s})+\mathrm{Js}^2} = \frac{l_1s^3 + l_2s^2 + l_3s + l_4}{(\mathrm{s}-\mathrm{j}0.3899)(\mathrm{s}+\mathrm{j}0.3899)(\mathrm{s}+0.1018)(\mathrm{s}+0.0538)(\mathrm{s}+0.0011)} \tag{65}$$

$$= \frac{A}{s-s_1} + \frac{B}{s-s_2} + \frac{C}{s-s_3} + \frac{D}{s-s_4} + \frac{E}{s-s_5} \tag{66}$$

$$A = -j0.3666$$
$$B = j0.3666$$
$$C = -2.9253*10^{-16}$$
$$D = 6.754*10^{-17}$$
$$E = -7.8382*10^{-18} \tag{67}$$

$$\frac{1}{T_1(\mathrm{s})+\mathrm{Js}^2} = -j0.3666e^{j0.3899t} + j0.3666e^{-j0.3899}$$
$$+(2.9253*10^{-16})\,\mathrm{e}^{-0.1018t} + (6.754*10^{-17})\,\mathrm{e}^{-0.0538t}$$
$$+(-1.8382*10^{-18})\,\mathrm{e}^{-0.011t} \tag{68}$$

$$D(\mathrm{t}) = \mathrm{F}_3(t)*L^{-1}\left(\frac{1}{T_1(s)+Js^2}\right) = \int(-1.45*10^3 + 543\tau - 0.0127\tau^2)(\mathrm{j}0.3666(\mathrm{e}^{-j0.3899(\mathrm{t}-\tau)} - \mathrm{e}^{j0.3899(t-\tau)}))\,\mathrm{d}\tau \tag{69}$$

$$I_1 = \int_0^t \sin(0.3899(\mathrm{t}-\tau))*(-1.45*10^3)d\tau$$
$$= \frac{1.45*10^3}{0.3899}\cos(t) - \frac{1.45*10^3}{0.3899} \tag{70}$$

$$I_2 = \int_0^t \sin(0.3899(\mathrm{t}-\tau))543\tau\,\mathrm{d}\tau \tag{71}$$

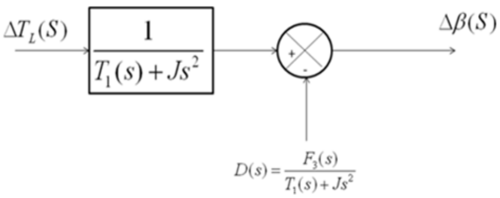

Fig. 3: Block diagram representation of the system with disturbance function D (s)

$$= 543(\frac{t}{0.3899}) - \frac{\sin(0.3899t)}{0.3899^2}$$

$$I_3 = \int_0^t \sin(0.3899(t-\tau))(-0.0127\tau^2)\,d\tau$$

$$I_3 = -0.0127(\frac{t^2}{0.3899} + \frac{2}{0.3899^3} + \frac{\cos(0.3899(t-\tau)}{0.3899^2}) \tag{72}$$

$$D(t) = 0.7332(\frac{1.45*10^3}{0.3899}(\cos(0.3899t)-1) +$$
$$543(\frac{t}{0.3899} - \frac{\sin(0.3899\,t)}{0.3899}) -$$
$$0.0127(\frac{t^2}{0.3899} + \frac{2}{0.3899}(\frac{\cos(0.3899t)}{0.3899^2} - \frac{1}{0.3899^2}))) \tag{73}$$

RESULTS AND DISCUSSION

The expression for D (t) in Eq. (73), demands some numerical calculations such that the different aspects of D (t) contributing to overall action of synchronous motor cane be realized. This particular philosophy forces the authors to present the results in graphical forms in Fig. 4 to 6. Furthermore the philosophy of calculation and extended results lead to the presentation in Fig. 7 and Table 1.

Figure 4 explains the variation of magnitude of the disturbance function D (t) against time at a particular value of slip of 0.15. From the nature of the problem formulation it is already well known that the asynchronous behavior of the synchronous machine in motor mode basically can be looked upon as a disturbance phenomenon; even though this should not be treated as a negative one because it indicates basically the starting method of synchronous motor. However qualitative treatment always does not guarantee the quality of a research work. As a supporting point to this statement the variation of D (t) is plotted against time in Fig. 4. From this it is very clear that ,out of all the terms, the coefficient associated with the term 't^2' is dominant. That is why the plot in Fig. 4, is observed as an increasing function. Furthermore the oscillations superimposed on the straight line (strictly speaking it is a parabola) in Fig. 4 basically indicates the involvement of sinusoidal function of time in the expression for D (t) and in reality exactly it is happening so far as the formulation is concerned. Figure 5 represents a family of plots of D (t) against time for different values of slips.

Figure 6 shows the variation of disturbance function D (t) with respect to slip at different time instants. From the expressions for D (t) it is quite

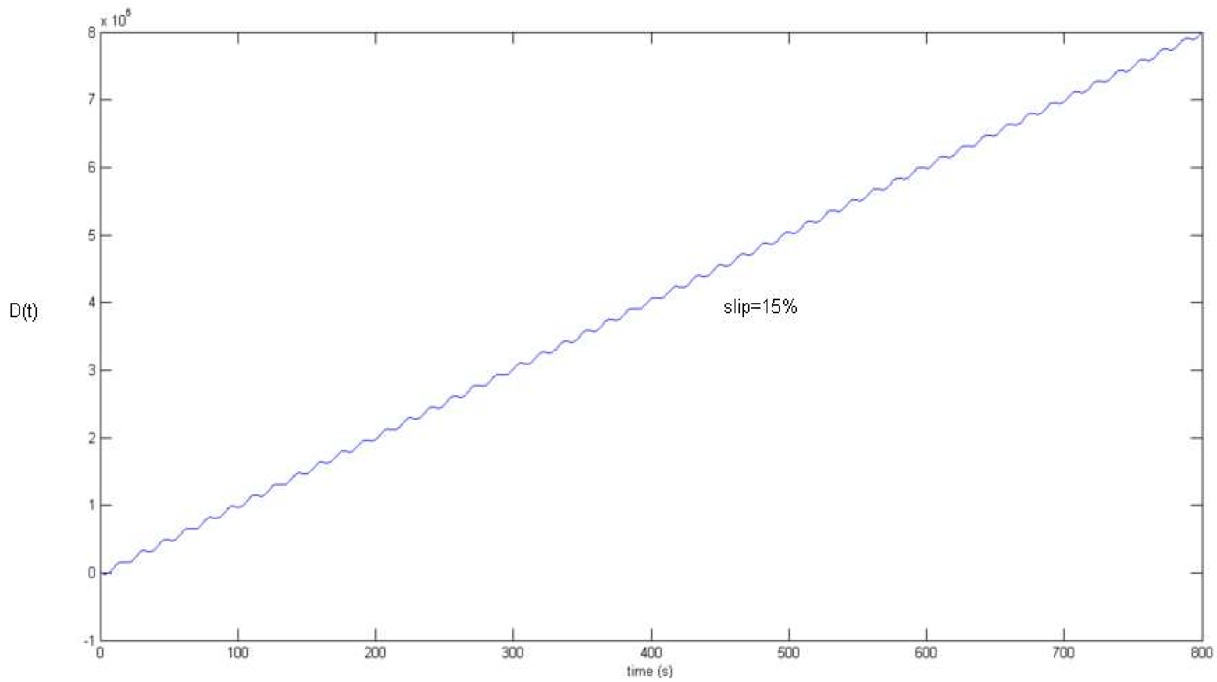

Fig. 4: Disturbance function D (t) vs. time

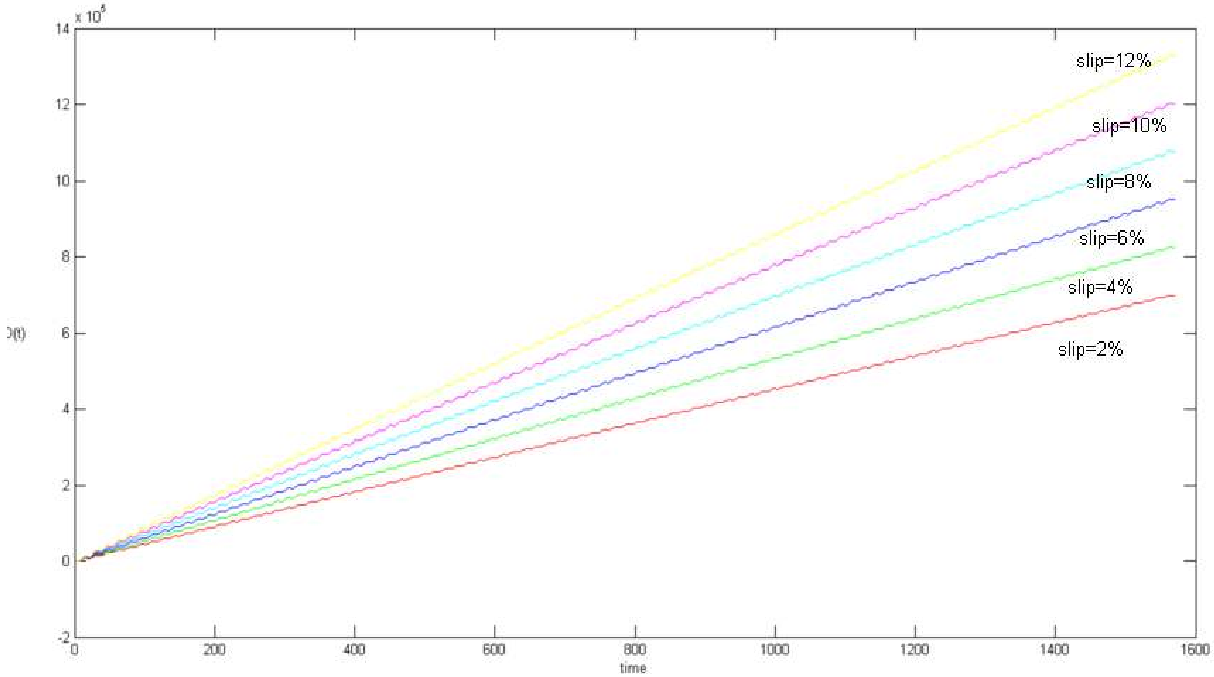

Fig. 5: D (t) vs. time for various values of slip

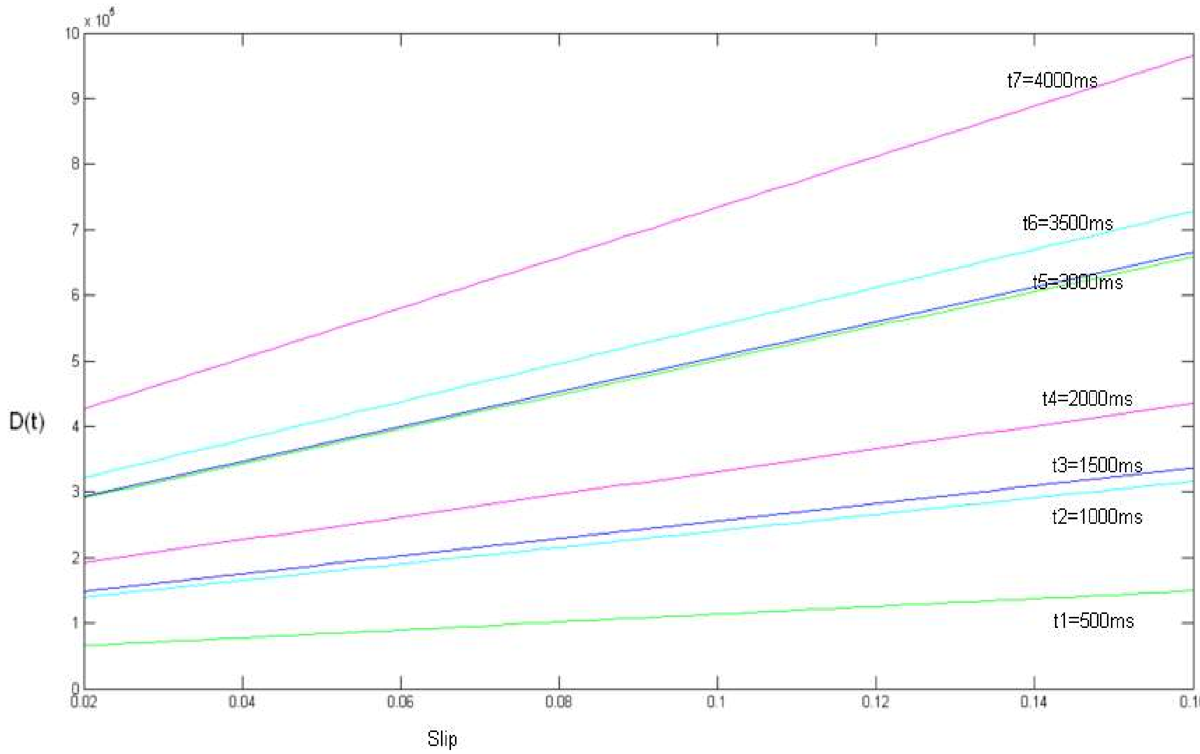

Fig. 6: Variation of magnitude of D (t) against slip for a fixed time instant

natural that oscillations will be superimposed on straight line nature. As seen from the expressions for involved co-efficients for D (t), it is clear that the term 'slip' (s_1) appears in the numerator of the concerned expressions, expressed as fractional terms. Hence the nature of the profile shown in Fig. 6 resembles with the physical fact. One interesting point is to be noted that the effect of oscillations superimposed on the profile of straight line have been observed in the Fig. 4 to 6 and accordingly all the physical conclusions/inferences

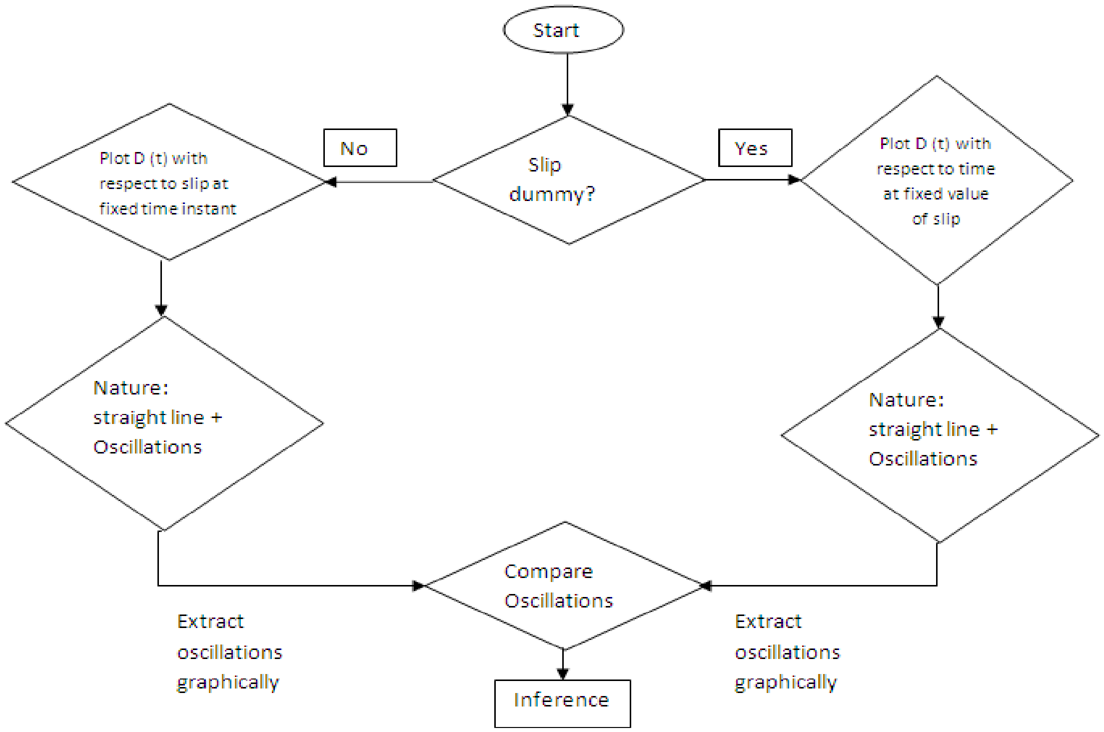

Fig. 7: Flow chart pertaining to contributions of oscillations to the responses in Fig. 4 to 6

Table 1: Numerical value of ∫D (t) dt over selected time spans

	1^{st} cycle	1^{st} cycle+2^{nd} cycle	1^{st} cycle+2^{nd} cycle+3^{rd} cycle
∫D (t) dt	0.2042	0.8168	1.8377

have been drawn in the above said paragraphs with sufficient engineering explanations. However the authors reveal that the mathematical nature of D (t) can be looked upon as a function of multivariable as 't' (time instant) and 's_1' (slip). Hence strictly speaking D (t) can be looked upon as the function D (s_1, t). Now is the question arises how to look the oscillations contributed by 'time' and 'slip' variations. This whole philosophical concept can be expressed in the form of a self explanatory flow chart given in Fig. 7.

Additional interesting facts about the results: With reference to Fig. 3, it is clearly observed that the role of D (s) can be looked upon as a transformed noise or disturbance function. For a control model of any system, it is very logical to observe the integrated value of the noise function in time domain for the sake of maintaining the health of the system. Based on this idea, Table 1 has been developed, which shows the numerical value of ∫D (t) dt over selected time spans.

The subsequent further explanations related to the Table 1, are as follows: It is difficult to infer about the nature of D (t) vs. time because the dominance of algebraic terms over trigonometric term are not observable at the first glance. Furthermore, relative dominance within the algebraic terms are also not understood from the expressions for D (t). That is why the integral effect of D (t) over time are calculated and it shows the existence of dominance of specific algebraic term. i.e., 't^2'. The reason behind the calculation of integrated values of D (t) over time (first cycle, first and second cycle and first, second and third cycles) is mainly to observe the integrated effect of noise during the sub transient period. Strictly speaking when the machine behave as an induction motor, the terminology, "sub transient period", has not much physical significance. But this terminology is used intentionally to emphasize the fact that it is not an isolated induction machine, rather it is a part of the full synchronous machine which has a damper winding being mainly responsible for creating sub transient state.

CONCLUSION

During the transition zone the synchronous motor is started as an induction motor with the help of damper winding. During the transition in order to avoid George's phenomenon the field winding of the synchronous motor is closed through an external resistance which is about 6-7 times that of the field winding resistance value. During the start of the above said process the change in voltage across the field winding is given by 220+s_1k where s1 is the slip of the induction motor and k is a constant. At start slip = 1, hence ΔU_f = 220 + s_1k is maximum. As the slip decreases towards 0, ΔU_f decreases towards 220. When this happens the field flux gets weakened as the slip movers from $s_1 = 1$ to $s_1 = 0$. This in turn decreases the electromagnetic torque developed in the machine for a fixed value of β (load angle). Hence T_e-T_L will also decrease during this process. This will reduce the rate of change of ω with respect to time in the motor. To adjust the decreased ω the β of the machine will have to increase accordingly to stabilize the system. Hence during the transition period Δβ will have to increase as slip goes from 1 to 0.

LIST OF SYMBOLS

i_d = Current in the D coil in p.u.
i_q = Current in the Q coil in p.u.
i_f = Current in the F coil in p.u.
i_{kd} = Current in the d axis damper coil (KD) in p.u.
i_{kq} = Current in the q axis damper coil (KQ) in p.u.
L_d = Self-inductance of D coil in p.u.
L_q = Self-inductance of Q coil in p.u.
L_{md} = Mutual inductance along d axis in p.u.
L_{mq} = Mutual inductance along q axis in p.u.
L_{ff} = Self-inductance of F (Field) coil in p.u
R_f = Resistance of the F (Field) coil in p.u.
L_{kd} = Self-inductance of the KD coil in p.u.
R_{kd} = Resistance of the KD coil in p.u.
L_{kq} = Self-inductance of the KQ coil in p.u.
R_{kq} = Resistance of the KQ coil in p.u.
β = Angle between the field (rotor) m.m.f. axis and armature (stator) m.m.f. axis

The machine data are given as (Ma *et al*., 2006):
J = 8 p.u.
L_d = 1.17 p.u.
L_{md} = 1.03 p.u.
L_q = 0.75 p.u.
L_{mq} = 0.61 p.u.
L_{kkd} = 1.122 p.u.
L_{kkq} = 0.725 p.u.
L_{ff} = 1.297 p.u.
R_{kd} = 0.03 p.u.
R_{kq} = 0.039 p.u.
R_f = 0.0015 p.u.

- When machine is at load:

i_s = 1 p.u.
i_{f0} = 0.97 p.u.
i_{kd0} = 0 p.u.
i_{kq0} = 0 p.u.
β_0 = 10^0

- When machine is at no load:

i_s = 0.1 p.u.
i_{f0} = 0.9 p.u.
i_{kd0} = 0 p.u.
i_{kq0} = 0 p.u.
β_0 = 0^0

REFERENCES

Al-Ohaly, A.A., R.M. Hamouda and M.A. Badr, 1997. Torsional oscillation associated with starting of three phase synchronous motors from a single phase supply. IEEE T. Energ. Convers., 12(1): 10-16.

Chattopadhyay, A.B., T. Sunil and C. Ruchira, 2011. Analysis of steady state stability of a Csi fed synchronous motor drive system with damper windings included. Trends Appl. Sci. Res., 6: 992-1005.

Das, J.C. and J. Casey, 1999. Characteristics and analysis of starting of large synchronous motors. Proceeding of the IEEE Commercial Power Systems Technical Conference on Industrial and Amp.

Gordon, R.S., B.D. Shashi and W.A.W. James, 1974. Synchronous motor drive with current-source inverter. IEEE T. Ind. Appl., IA-10(3): 412-416.

Isfahani, A.H. and S. Vaez-Zadeh, 2011. Effects of magnetizing inductance on start-up and synchronization of line-start permanent-magnet synchronous motors. IEEE T. Magn., 47(4): 823-829.

Knight, A.M. and C.I. McClay, 2000. The design of high-efficiency line-start motors. Proceeding of the 34th IAS Annual Meeting, Industry Applications Conference, Conference Record of the 1999 IEEE, 1: 516-522.

Ma, X., S. Ding and W. Li, 2006. Calculation and analysis of magnetic fields and temperature fields for salient pole synchronous motors in the process of starting. Proceeding of the International Conference on Power System Technology, pp: 1-6.

Marx, D., S. Pierfederici and B. Davat, 2008. Nonlinear control of an inverter motor drive system with input filter-large signal analysis of the DC-link voltage stability. Proceeding of the IEEE Power Electronics Specialists Conference (PESC, 2008). Rhodes, USA, June 15-19, pp: 498-503.

Najafi, S. and N.C. Kar, 2007. Effect of short-circuit voltage profile on the transient performance of saturated permanent magnet synchronous motors. Proceeding of the IEEE Power Engineering Society General Meeting. Tampa, FL, June 24-28, pp: 1-6.

Sergelen, B., 2007. Mathematical model of salient pole synchronous motors supplied by a frequency converter. Proceeding of the International Forum on Strategic Technology (IFOST, 2007). Ulaanbaatar, pp: 390-393.

Wang, X. and N. Ren, 2003. Simulation of asynchronous starting process of synchronous motors based on Matlab/Simulink. Proceeding of the 6th International Conference on Electrical Machines and Systems (ICEMS, 2003), 2(1): 684-687.

Weifu, L., L. Yingli and Z. Haisen, 2012. Influences of rotor bar design on the starting performance of line-start permanent magnet synchronous motor. Proceeding of the 6th International Conference on Electromagnetic Field Problems and Applications (ICEF, 2012), pp: 1-4.